International Journal of Basic and Applied Sciences, 14 (4) (2025) 533-548

International Journal of Basic and Applied Sciences

Website: www.sciencepubco.com/index.php/IJBAS
https://doi.org/10.14419/snte6g31
Research paper

Development of A PLC-Based Automated Test System for The Life Cycle Evaluation of The Caster Wheel Brake Mechanisms in Medical Devices

Harsh Dilip Kene [1], Sudhir Madhav Patil [2] *, Prasenjit Guru [3], Piyush Dipak Bachhav [4]

[1] *Student, Second Year M. Tech.: Mechatronics, Department of Manufacturing Engineering and Industrial Management, COEP Technological University (COEP Tech), Chhatrapati Shivajinagar, Pune: 411005, Maharashtra State, India*
[2] *Associate Professor, Department of Manufacturing Engineering and Industrial Management, COEP Technological University (COEP Tech), Chhatrapati Shivajinagar, Pune: 411005, Maharashtra State, India.*
[3] *Reliability and Compliance Architect, Ultrasound Research and Development, Philips Healthcare Innovation Center (HIC), Philips India Limited, Baner, Pune: 411045, Maharashtra State, India.*
[4] *Student, Second Year M. Tech.: Project Management, Department of Manufacturing Engineering and Industrial Management, COEP Technological University (COEP Tech), Chhatrapati Shivajinagar, Pune: 411005, Maharashtra State, India*
**Corresponding author E-mail: smp.prod@coeptech.ac.in*

Received: July 1, 2025, Accepted: August 12, 2025, Published: August 20, 2025

Abstract

Caster wheels used in medical devices such as ultrasound systems are critical for mobility and safety. Their brake mechanisms must maintain performance over repeated use. This study aims to develop and implement a Programmable Logic Controller (PLC)-based automated test system to evaluate the life cycle performance of caster wheel brake mechanisms under accelerated testing conditions. A dedicated mechatronics test setup was designed incorporating a pneumatic actuator, proximity sensor, and strain gauge for real-time monitoring and control. A fixture was developed to simulate repeated brake engagement and disengagement cycles using a single pneumatic cylinder. The PLC controlled the test sequence and recorded sensor feedback, while manual force measurements were taken at specific intervals up to the designated cycles corresponding to the life cycles of the braking mechanism, C_L. The caster wheel brake engagement and disengagement forces were measured across eleven distinct test instances: 0, $0.1C_L$, $0.2C_L$, and so on up to C_L. These tests were conducted over ten intervals. The measured forces showed consistent results, with variations limited to within ±2% of the required rated values for both engagement and disengagement. This indicated minimal wear or loss in functionality over C_L. The system operated reliably for C_L continuous cycles, validating the mechanical robustness of both the test rig and the caster wheel components. This automated system offers a time-efficient solution for reliability testing of the braking mechanism of the caster wheel. However, the present study focuses on the caster wheel used in the medical equipment manufacturing sector. It enables consistent testing without human intervention, ensuring better quality assurance and predictive maintenance insights. The developed PLC-based test system provides a reliable platform for life cycle evaluation of caster wheel brake mechanisms. Its modular design and automation capability make it adaptable for testing various wheel types and supporting further research in reliability engineering.

Keywords: *Caster Wheel Brake Mechanism; Life Cycle Testing; Mechatronics Test System; Medical Device Component Reliability; PLC-Based Automation.*

1. Introduction

In the modern era of healthcare and advanced medical technologies, mobility and stability in medical equipment are of paramount importance. Medical devices such as ultrasound machines, diagnostic carts, wheelchairs, and patient monitoring systems often rely on caster wheels for ease of movement and repositioning. The performance of these caster wheels, especially their braking mechanisms, directly affects the safety, usability, and reliability of the equipment. In high-stakes environments like hospitals, the failure of a brake mechanism can result in equipment instability, patient safety hazards, or even device malfunction [1-3]. Therefore, a systematic evaluation of the performance and durability of caster wheel brake mechanisms under real-world operating conditions is essential.

Reliability testing of mechanical components traditionally involves manual methods, which are not only labor-intensive but also prone to inconsistencies. In recent years, automated test systems using Programmable Logic Controllers (PLCs) have emerged as robust solutions for life cycle evaluation of various electromechanical systems. PLCs offer enhanced precision, repeatability, and control, enabling complex automation with real-time feedback and safety features. Incorporating mechatronic principles - combining mechanical, electrical, and control systems - these setups allow for the replication of actual working conditions in a controlled environment [4].

In the domain of caster wheels, however, limited research has been conducted on developing standardized, automated test systems specifically designed for assessing the life cycle performance of brake mechanisms. Most studies in the literature focus on material wear, rolling

resistance, and general mechanical integrity of caster wheels [5-8] but lack a targeted evaluation of the braking function under cyclic loading conditions.

Several researchers have explored reliability testing frameworks in different mechanical contexts. For example, a lab-based mechatronic test setup compared thermoplastic bushings and ball bearings in wheelchair casters, showing higher durability and cost-effectiveness for thermoplastics under accelerated wear conditions [8]. A pneumatic door slam testing system controlled by a PLC was developed to assess the strength and performance of vehicle doors, highlighting the role of automation in reliability testing [9], [10]. A simulation-based mechatronic approach was used to design and prototype an electromechanical actuation system for a medium-voltage vacuum contactor, integrating mechanical, electromagnetic, and control subsystems [11]. Although such frameworks are valuable, they cannot be directly applied to testing the brake mechanisms of caster wheels used in medical devices. These mechanisms function under unique constraints. They must meet high safety and reliability standards. The design needs to be compact and lightweight. The operation should be simple and quick. Additionally, they must withstand frequent use and regular relocation.

In terms of test automation and feedback systems, the integration of sensors like proximity sensors/switches and strain gauges has enabled precise cycle counting and force measurement in various industrial testing applications [12], [13]. These sensors are crucial for ensuring accurate detection of end-to-end states of the actuator responsible for the caster wheel brake's engagement and disengagement states, a requirement particularly critical when evaluating the functionality of mechanical brakes. Sensor-based feedback loops in pneumatic testing systems have improved both safety and efficiency, making them suitable for continuous unattended operation [14].

Another relevant area of investigation involves pneumatic actuation for mechanical testing. Pneumatics offer a cost-effective, easily controllable means of applying linear forces, which are ideal for simulating manual actions like brake engagement. Research has shown that pneumatic cylinders enable consistent force application in high-cycle durability testing, with PLC control and sensor feedback enhancing test reliability and automation efficiency in component evaluation setups [15], [16].

Recent advancements in automated testing systems have emphasized the integration of sensor-based monitoring, machine learning algorithms, and real-time data acquisition to enhance reliability evaluation in mobility components, including caster wheels. Studies in [5], [17], [18] demonstrated the application of automated load–load-displacement tracking and vibration profiling to predict early-stage wear in caster assemblies under dynamic operating conditions. Similarly, Mane et al. [17] introduced a closed-loop automated endurance test rig capable of simulating multi-directional movement patterns and variable floor surfaces, replicating real-world stresses more accurately than traditional static tests. For reliability under dynamic loads, recent works such as [19], [20] have combined accelerated life testing with finite element fatigue modelling to identify design-critical zones in wheel hubs and swivel mechanisms. These developments underline the growing emphasis on high-fidelity, automated test methodologies that align with the evolving performance demands in industrial and medical caster applications, providing a strong technical backdrop for the present study.

While prior studies have extensively explored caster wheel testing [5], [6], PLC-based automation [9], [10], and pneumatic actuation systems [14-16], there remains a significant research gap in evaluating these systems under dynamic, real-world operating conditions. Dynamic testing poses unique challenges, including variable load distribution, complex motion trajectories, and the integration of real-time sensing for predictive fault detection [21], [22]. Furthermore, PLC-based platforms, though robust and widely adopted in industrial automation, can exhibit limitations in flexibility and cost-effectiveness when compared to microcontroller-based or IoT-enabled architectures [23]. Recent advancements post-2022 have introduced hybrid systems that integrate PLC reliability with IoT-driven analytics, enabling remote monitoring, adaptive control, and machine learning–based fault prediction [24-27]. These developments highlight an emerging opportunity to bridge the gap between conventional automated testing setups and smart manufacturing environments, where dynamic adaptability and predictive capabilities are critical for ensuring caster wheel performance and reliability.

Despite these advancements, no comprehensive study has yet focused on the development of a dedicated PLC-based automated system tailored for life cycle evaluation of caster wheel brake mechanisms, especially in medical devices. Given the growing demand for mobile healthcare equipment and the need to comply with stringent regulatory standards, such a study is both timely and necessary.

To address this gap, the present research focuses on designing, developing, and validating an automated mechatronics test system using a PLC for evaluating the life cycle of caster wheel brake mechanisms. The system integrates a 200 mm stroke double-acting pneumatic cylinder mounted in a vertically inclined position, proximity sensors for positional feedback, and a strain gauge setup for real-time force monitoring. The test setup is designed to perform continuous cyclic testing, where one cycle includes both engagement and disengagement of the brake mechanism. This configuration enables simulation of actual operating conditions to assess long-term reliability.

The most used caster wheel model was selected for testing. This wheel is prevalent in the medical industry and represents the desired design philosophies in brake construction. The developed fixture is adjustable and robust, accommodating different wheel geometries and ensuring consistent alignment and force application. This ensures accurate and repeatable results over thousands of cycles.

The force required for brake engagement and disengagement was recorded continuously using a data acquisition system. This data was sent as an analog input to the PLC. To ensure accuracy, the recorded force was also manually verified using a force gauge at specific intervals during the brake mechanism's life cycle (i.e., 0, $0.1C_L$, $0.2C_L$, ..., C_L). The readings were analyzed to detect variations and infer whether the caster wheel brake mechanism can function effectively and reliably over the intended life of C_L. This further helps to infer mechanical wear, slippage, or degradation.

The purpose of this research is to carry out accelerated testing using an automated test setup. The testing focuses on evaluating the performance of the caster wheel brake mechanism over a specified number of cycles, C_L. Based on this, the number of specified or successful cycles, whichever is minimum, is considered as the service life of the brake mechanism under defined conditions. The same test setup can be further used for brake mechanism failure analysis, which is beyond the scope of this study. However, the test was not extended beyond the C_L cycle limit. Within C_L, the test aimed to observe any signs of brake mechanism failure. The purpose was to gain preliminary insights into the design limits of the brake components.

If the brake engagement and disengagement force value falls outside ± 3% of the respective rated force during any C_L then the situation is considered as failure of the braking mechanism. The data suggests that the selected caster wheel model maintained its functional integrity within the specified life cycle, validating the robustness of its brake systems and the efficacy of the developed test setup.

The broader application of this research lies in its potential to serve as a standardized methodology for life cycle evaluation of the braking mechanism of caster wheels used in medical and industrial environments. The test system, being fully automated, offers substantial advantages in terms of time efficiency, data accuracy, and repeatability. The setup also allows for future scalability, including testing under variable loads or adapting to other mechanical components requiring cyclic endurance evaluation.

The rest of the paper is organized as follows: Section 2 presents the Materials and Methods, describing the components used, system architecture, and testing procedures. Section 3 discusses the Results and Discussion, including the force analysis, system performance, and durability findings. Finally, Section 4 concludes the study, highlighting the limitations, contributions, and suggesting avenues for future research.

2. Materials and methods

This section outlines the detailed approach adopted in developing and deploying a PLC-based automated system for testing the life cycle performance of brake mechanisms in caster wheels used in medical equipment. The procedures described below are organized into subsections covering materials selection, mechanical fixture development, automation and control integration, instrumentation setup, data acquisition, experimental procedure, and validation trials. This comprehensive methodology ensures repeatability and reliability in the test setup and its findings.

2.1. Materials and components

2.1.1. Caster wheels

A model of a medical-grade caster wheel, as shown in *Figure 1,* was selected for this study. Due to confidentiality and intellectual property rights (IPR) considerations, the specific make and model of the caster wheel used in this study cannot be disclosed. However, the caster wheel represents a commercially available variant commonly used in medical equipment applications, featuring a mechanical brake mechanism. All relevant functional and performance parameters necessary for testing and evaluation have been included in the study. This caster wheel has a feature of a two-in-one bi-brake system: this system combines two locking features - directional lock (DL) and total lock (TL) - within a single caster. The DL (green pedal) helps maintain straight-line movement when needed, while the TL (red pedal) provides secure parking with a single press. Releasing both locks allows for smooth lateral movement and effortless turning in confined areas. The caster wheel has a diameter of 125 mm and a width of 32 mm. Each wheel has a load capacity of 100 kg. These wheels were chosen to reflect the most commonly used designs in ultrasound systems and similar medical diagnostic equipment.

Fig. 1: The Castor Wheel Considered for Study.

2.2. Design and development of the test fixture

The mechanical fixture serves as the interface between the actuation system and the caster wheel. It was engineered to position the wheel in a fixed orientation while applying force on the brake lever to simulate real-world caster wheel brake engagement and disengagement conditions responsible for locking and unlocking, respectively.

2.2.1. Fixture design objectives

The test fixture, illustrated in *Figure 2*, was specifically designed to meet several functional objectives. It ensures repeatable positioning and precise alignment of the caster wheel throughout the testing process. The structure is rigidly constructed to prevent any deflection during operation, maintaining consistent test conditions. It is also adaptable to accommodate various caster wheel brake geometries, making it suitable for testing different designs. In addition, the fixture allows for quick and easy mounting and removal of the caster wheel specimen, enhancing operational efficiency. The mechanical layout of the fixture includes designated mounting slots for securing the caster wheels and features a vertical orientation for the actuator cylinder, as depicted in *Figure 2*.

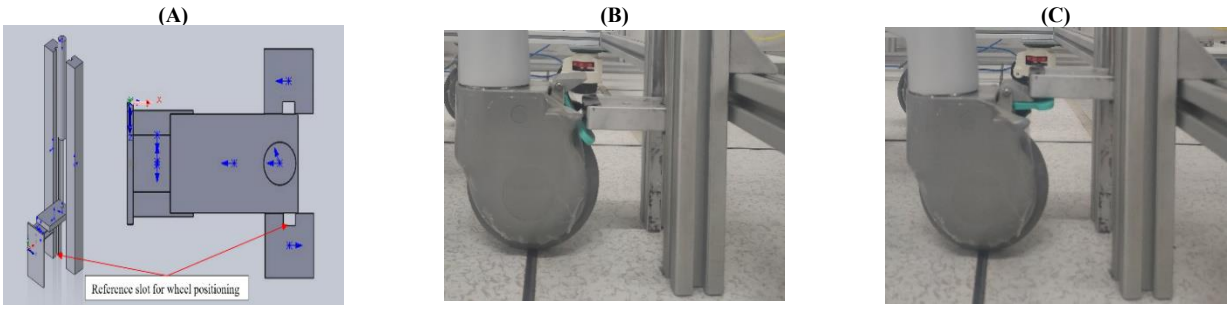

Fig. 2: The Developed Test Fixture (A) CAD Model (B) Actual - Engagement State (C) Actual - Disengagement State

2.2.2. Pneumatic actuation mechanism

A double-acting pneumatic cylinder with a 200 mm stroke length was selected for the testing setup. The cylinder was mounted in a vertical orientation to apply a consistent downward force on the brake mechanism. The schematic diagram of the test setup presented in *Figure 3* illustrates the contact points involved during the running phase of the test. Table 1 details the distance of all three pedals (release, DL, and TL) from the ground and the cylinder's retracted end plate position under different conditions.

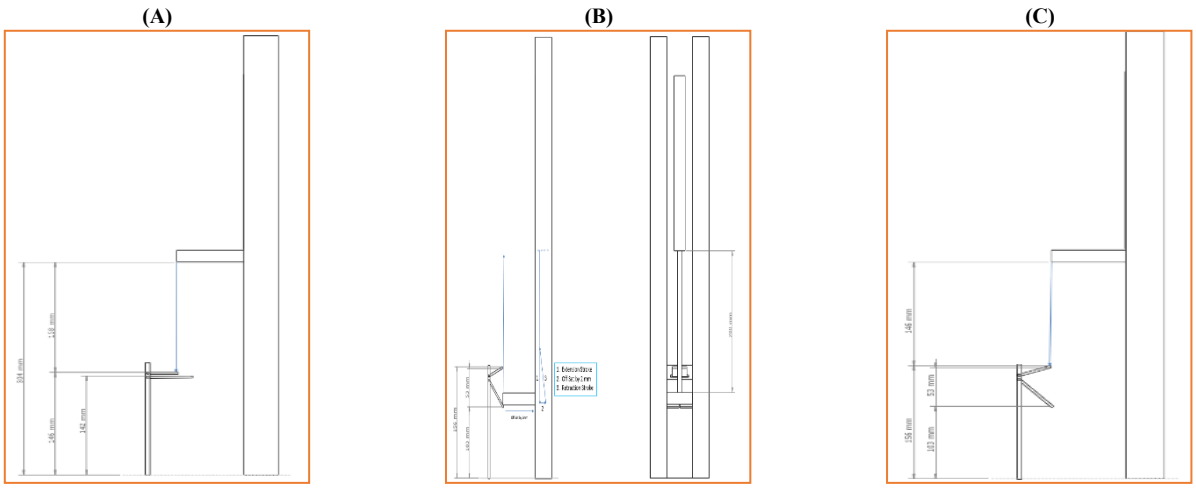

Fig. 3: Schematic of the Test Setup, Elaborating the Contact Points (A) Before Commencement of the Test (B) After First Time Extension (C) After Last Cycle Retraction.

Table 1: Details Of the Distance of All Three Pedals

Pedal Type	Scenario	Distance from the Ground	Distance from home position of the actuator (i.e., when retracted)
Unlock/Release Brake Pedal	When brakes are not applied	146 mm	158 mm
	When the brakes are applied	156 mm	146 mm
DL and TL pedal	When brakes are not applied	142 mm	162 mm
	When the brakes are applied	103 mm	200 mm

The castor wheel operates in two primary states. When the brakes are not engaged, all pedals are in a horizontal position, denoted by the symbol '='. When the brakes are applied, the pedals tilt in opposite directions, represented by the symbol '<'. Initially, the castor wheel is placed on the fixture with all locks disengaged (=).

As the test begins, the actuator extends. The end plate at the end of the actuator rod first contacts the release brake pedal, but since the brake is already disengaged, this has no immediate effect. As the extension continues, the end plate then meets the DL (green) and TL (red) pedals, which engage the brakes. This causes the unlock/release brake pedal to lift and rotate slightly, shifting the status to '<'.

Table 2 outlines the sequence of contact and force measurement points during the actuator's extension. The reader is requested to read Table 2 as per the reading order number to understand the sequence of contact. At 146 mm, the end plate contacts the release brake pedal (assuming the brakes are applied), causing the brakes to disengage and the pedals to return to their horizontal position ('='). At 162 mm, the end plate reaches both lock pedals, and by 200 mm, they are fully engaged, braking the castor wheel. Thus, one complete extension of the cylinder includes brake release followed by re-engagement over the full 200 mm stroke.

During the return stroke, no braking activity occurs. The actuator plate is guided back via a 2 mm offset path, enabled by specially designed grooves in the guideways. This lateral shift occurs at the fully extended 200 mm position, initiated by side forces acting on the plate.

Table 2: Details Of Contact Points and Force Measurement Points During the Extension Stroke

End plate position w.r.t. home position in mm	Reading order	Contact Point	Force Measurement Point	Reading order	Contact Point	Force Measurement Point
		During the First Cycle, as the test initiates			During the running phase, post the first cycle	
0	1	No	No	6	No	No
146	2	No	No	7	Release the Brake Pedal	Yes, initiates unlocking by experiencing a sudden heavy force required for unlocking
158	3	Release Brake Pedal	Yes, but not important as the brake was not applied and the caster wheel was positioned in a free state.	8	Release the Brake Pedal	Yes, end of unlocking as the pedal takes a horizontal position
162	4	Both lock pedals	Initiates the braking	9	Both lock pedals	Yes, initiates locking by experiencing the sudden force required for pressing the locking pedal.
200	5	Both lock pedals	Completes braking	10	Both lock pedals	Completes braking

Note: The Reader is advised to read Table 2 as per the reading order number to understand the sequence of contact.

To regulate the actuation force, a pneumatic flow control valve was used, allowing precise adjustment of stroke speed. The test fixture was constructed using high-strength mild steel and aluminum, offering a balance between structural rigidity and reduced weight. Linear bearings and guide rails ensured accurate actuator plate movement and minimized lateral loads on the brake pedals.

2.3. Control and automation system

2.3.1. PLC selection and configuration

A PLC was selected to control the entire test cycle. The PLC received input from a proximity sensor and a strain gauge and controlled the actuation of the pneumatic cylinder via an output relay. Table 3 presents the number of input and output signals and their type.

Table 3: List of Inputs/Outputs (I/Os) to and from the PLC.

Sr. No.	Description	Input/Output	Field Device / HMI	Position	Type
1	START BUTTON (Manual Push Button) to start the test	Input	Field Device	On the Control Panel Cabinet	Digital (Binary)
2	START BUTTON to start the test	Input	HMI	HMI Control Screen	Digital (Binary)
3	STOP BUTTON (Manual Push Button) to stop the test	Input	Field Device	On the Control Panel Cabinet	Digital (Binary)
4	STOP BUTTON to stop the test	Input	HMI	HMI Control Screen	Digital (Binary)
5	EMERGENCY STOP BUTTON (Manually Operated) to stop the test due to an emergency	Input	Field Device	On the Control Panel Cabinet	Digital (Binary)
6	EMERGENCY STOP BUTTON to stop the test due to an emergency	Input	HMI	HMI Control Screen	Digital (Binary)
7	RESET BUTTON to reset the test system and controller so that a fresh test can be initiated.	Input	Field Device	On the Control Panel Cabinet	Digital (Binary)
8	RESET BUTTON to reset the test system and controller so that a fresh test can be initiated.	Input	HMI	HMI Control Screen	Digital (Binary)
9	Proximity Sensor (Reed Switch) for Retracted Position Detection (mounted at 0 mm)	Input	Field Device	On a cylindrical body	Digital (Binary)
10	Proximity Sensor (Reed Switch) for Extended Position Detection (mounted at 200 mm)	Input	Field Device	On a cylindrical body	Digital (Binary)
11	Strain Gauge for Force Value Measurement	Input	Field Device	Below the end plate that is attached to the end of the piston rod.	Analog
12	Set the Number of Cycles for the experiment	Input	HMI	HMI Control Screen	Digital (Discrete other than Binary)
13	Relay Coil for actuating solenoid mounted on the 5/2 Main Direction Control Valve	Output	Field Device	Mounted with Solenoid Solenoid-controlled 5/2 Direction Control Valve	Digital (Binary)
14	Number of Cycles completed	Output	HMI	HMI Display Screen	Digital (Discrete other than Binary)
15	Strain Gauge Force values for observation by the user	Output	HMI	HMI Display Screen	Digital

2.3.2. Sensor integration

A proximity sensor (reed switch) was installed on the cylinder body to detect the extreme positions - both retracted (home, 0 mm) and extended (200 mm) - of the actuation plate's movement. This sensor delivered real-time feedback to the PLC, enabling it to monitor the actuator's extension and retraction status accurately. Additionally, a strain gauge was mounted on the underside of the end plate. This gauge was integrated into a Wheatstone bridge configuration and connected to a load cell amplifier to improve signal clarity. The resulting analog signal was then fed into the PLC, allowing for continuous monitoring of the force required during testing.
Figure 4 represents the conceptual block diagram of the component integration of the test setup.

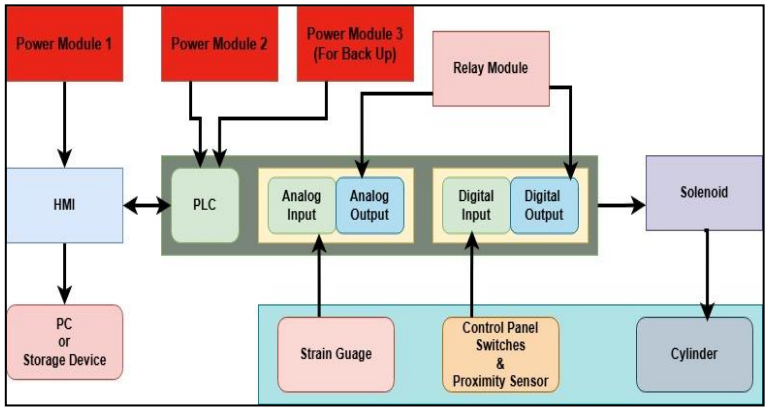

Fig. 4: PLC-Based Control Circuit Diagram.

2.3.3. Human-machine interface (HMI)

A basic graphical user interface (GUI) was developed for the HMI, as shown in *Figure 5,* to facilitate user interaction with the test setup. It enabled users to enter the required number of test cycles and provided a real-time display of both the ongoing cycle count and the force required during brake engagement. The GUI also included operational controls, allowing users to start, stop, reset the system, or activate an emergency stop when necessary. Communication between the GUI and the PLC was established through an Ethernet connection, ensuring reliable data exchange. The interface was also configured to periodically update and store data logs for further analysis.

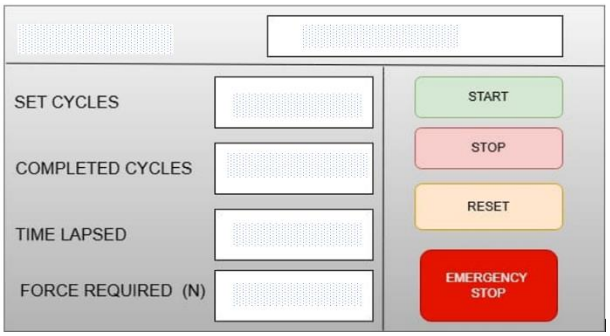

Fig. 5: Human-Machine Interface (HMI).

2.4. Force measurement and data acquisition

Force measurement was a critical parameter for evaluating the mechanical performance of the brake mechanism. The strain gauge setup was calibrated using standard weights, and the output voltage was mapped to force in Newtons.
Calibration Reference: Standard methods for strain gauge calibration were followed as outlined in the literature [28-30]. A linear calibration curve was developed and used for subsequent force readings.
Manual force measurements were also taken using a calibrated digital force gauge (range: 0-200 N) at intervals of 0, $0.1C_L$, $0.2C_L$, ..., C_L cycles to verify automated measurements. Table 4 presents the manual force measurement, as well as the strain gauge force recording schedule and sampling points (peak value) for verification.

Table 4: Manual Force Measurement Schedule and Sampling Points for Both Engagement and Disengagement Force Validation

Cycle No.	Prior Status	Pedal on which force is applied	Action Performed	Purpose	Nota-tion
0	Brakes not applied	DL and TL Pedal	Engagement for Braking (B)	To note the maximum force required to apply the brake	0B
1	Brakes ap-plied	Release Brake Pedal	Disengagement of Brakes, i.e., Releasing brakes (R)	To note the maximum force required to release the brake or unlock the wheel.	1R
1	Brakes not applied	DL and TL Pedal	Engagement for Braking (B)	To note the maximum force required to apply the brake	1B
$0.1C_L$	Brakes Ap-plied	Release Brake Pedal	Disengagement of Brakes, i.e., Releasing brakes (R)	To note the maximum force required to release the brake or unlock the wheel.	$0.1C_LR$
$0.1C_L$	Brakes not applied	DL and TL Pedal	Engagement for Braking (B)	To note the maximum force required to apply the brake	$0.1C_LB$
.	.	.		.	.
.	.	.		.	.
.	.	.		.	.
C_L	Brakes Ap-plied	Release the Brake Pedal	Disengagement of Brakes, i.e., Releasing brakes (R)	To note the maximum force required to release the brake or unlock the wheel.	C_LR
C_L	Brakes not applied	DL and TL Pedal	Engagement for Braking (B)	To note the maximum force required to apply the brake	C_LB

2.4.1. Hardware setup

Figure 6 depicts the hardware arrangement for force measurement. In the experimental setup, a strain gauge was employed on the downside of the end plate to measure the force required on the brake pedals. Since the strain gauge output consisted of very small resistance changes, a signal conditioning circuit was used to process the signal. This included a Wheatstone bridge configuration integrated with an instrumentation amplifier (INA125), which amplified the signal to a level suitable for further processing.
The conditioned analog signal was then interfaced with the PLC, which was responsible for acquiring the data. As the sensor was an analog type, analog input channels were utilized for signal acquisition. The PLC was programmed to convert the input signal into corresponding force values using a calibration equation derived from initial testing.
The HMI was connected to the PLC using Ethernet. The HMI displayed real-time force readings, enabling the operator to monitor system behavior visually and continuously.
To facilitate data logging, a personal computer (PC) was integrated into the setup for experimentation purposes, and the same can be replaced with a data storage device. The PC communicated with the PLC directly using OPC UA (Open Platform Communications Unified Architecture) to connect to the data logger. This configuration allowed for continuous logging of required force data through the strain gauge. The recorded data was stored in Microsoft Excel-compatible format, which could be retrieved in soft copy or printed as required by the user.

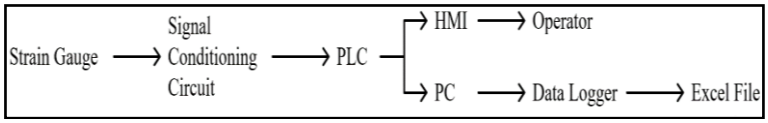

Fig. 6: Hardware Arrangement for Force Measurement.

2.5. Experimental procedure

2.5.1. Cycle definition

One complete cycle in the system comprised three sequential stages: disengagement, engagement, and return stroke.

- Disengagement: The cycle began with the downward movement of the pneumatic cylinder to operate the release brake pedal. This action led to the disengagement of the brakes, effectively releasing the braking mechanism.
- Engagement: As the cylinder continued its downward motion, it activated the DL and TL pedals, thereby engaging the brakes and applying them to the caster wheel.
- Return stroke: Once the cylinder had fully extended and the DL and TL pedals were pressed to their extreme positions, it initiated the return stroke. During this phase, the cylinder retracted by an offset distance of 2 mm and returned to its original home position.

The PLC was programmed to ensure that the next cycle would only begin automatically after the proximity sensor confirmed the successful completion of the previous cycle and verified whether additional cycles were required based on the preset number.

2.5.2. Test execution (event sequence description)

The system operation begins with its initialization, followed by the user setting the desired number of cycles through the GUI of the HMI. Once the configuration is completed, the process is initiated by pressing the START button, which is available either on the physical control panel cabinet or on the HMI screen.

Upon starting, the solenoid that controls the spring return 5/2 main direction control valve (mono stable) is energized, causing the actuator to begin its extension stroke. As the actuator extends, the end plate attached to the piston rod first meets the release brake pedal. At this point, the strain gauge - mounted just beneath the end plate - records the variation in force required, and the corresponding values are displayed in real-time on the HMI screen for user observation. This contact results in the release of the brakes and the unlocking of the caster wheel, bringing the system to an intermediate or '=' state.

The actuator continues its extension until the end plate contacts the DL and TL pedals. As these pedals are gradually pressed, the process of brake engagement begins. Once the actuator reaches its full extension, both DL and TL pedals are pressed completely, leading to full engagement of the brakes and locking of the caster wheel, thereby attaining the final '<' state. During this movement, the strain gauge - mounted just beneath the end plate – keeps recording the variation in force required, and the corresponding values are displayed in real-time on the HMI screen for user observation.

A proximity sensor (reed switch) mounted at the 200 mm mark on the cylinder body detects this fully extended position and confirms the successful extension stroke. Subsequently, the solenoid on the 5/2 direction control valve is de-energized, triggering the actuator to retract. During this return stroke, the line of action of the stroke of the actuator moves backward through a 2 mm offset distance, as shown in *Figure 3,* and eventually reaches its original retracted home position (0 mm). A second proximity sensor, placed at the 0 mm mark, verifies this retracted position.

The system first checks if the number of completed cycles is less than the preset cycle count. It then verifies whether the caster wheel brake engagement and disengagement force value recorded by the strain gauge falls within ±3% of the rated force required for engagement and disengagement of caster wheel brakes, respectively. This check is performed separately for both the force required for engagement and disengagement of the caster wheel brakes. If both conditions are met, the system loops back to initiate the next cycle. However, if the number of completed cycles matches the set count or if the strain gauge records a force outside ±3% of the respective rated force required, the system is automatically interlocked, preventing further operation. The system is also interlocked if either the STOP button or the EMERGENCY STOP button is activated from the operator control panel or via the HMI. *Figure 7* presents a flow chart of the test execution (event sequence description).

2.5.3. Data recording and safety

During operation, the system recorded all cycle counts along with their corresponding force readings in a CSV file format to enable easy data logging and post-processing. Safety was addressed through the integration of Emergency Stop functionality at both hardware and software levels, ensuring immediate system shutdown when required. Additionally, the system was programmed to halt automatically either upon reaching the predefined number of cycles or when a fault condition was detected. This stoppage could also be triggered manually through dedicated STOP controls available in both hardware and software interfaces, enhancing the overall reliability and safety of the setup.

2.6. Validation trials

To ensure the experimental setup performs reliably under cyclic conditions, a comprehensive series of validation trials supported functional integrity, force calibration, and system repeatability. These trials also determined the limiting force values necessary for effective brake disengagement and engagement using the release brake pedal and the DL and TL brake pedals, respectively.

A total of 200 trials, comprising 100 manual and 100 automated cycles, established a reference dataset. During manual testing, a digital force gauge captured force readings, while the automated trials employed a strain gauge integrated beneath the actuator's end plate. This sensor continuously monitored the force required during each operation, displaying real-time values on the HMI screen and simultaneously logging data to a connected PC or storage device. In both modes - manual and automated - the system captured peak forces required during each cycle's disengagement and engagement phases, which, as defined in Section 2.5.1, comprise disengagement, engagement, and return stroke.

The force outcomes for both modes were analyzed to confirm close alignment between manually observed and sensor-based measurements. These trials helped to finalize the rated peak force values for brake disengagement and brake engagement of the caster wheel. These served as thresholds for subsequent life cycle (C_L) testing. Any deviation beyond ±3% of these rated values is identified as abnormal, suggesting potential mechanical degradation that may compromise braking effectiveness. Persistent deviation from this range may indicate loosening or wear within the mechanism, eventually leading to braking failure.

The ±3% tolerance limit for brake engagement and disengagement force is based on practical engineering considerations. The test equipment used in this study offers high measurement accuracy, with force sensors capable of reliably detecting variations well below this threshold. In the absence of formalized standards governing acceptable force variation for caster wheel brakes in medical applications, this limit was defined based on internal benchmarking and industry practices. Discussions with domain experts and comparison with similar mechanical systems suggest that a ±3% variation does not impact functional performance or user safety, while larger deviations may indicate emerging mechanical issues. Therefore, this threshold serves as a conservative yet realistic criterion for identifying potential performance degradation.

The trials were not limited to checking the force calibration; they also focused on other important performance factors. The caster wheel mounting process maintained consistent alignment, ensuring repeatable contact during actuation. Fixture deflection was monitored to minimize structural distortion under the load. Pneumatic pressure and actuator stroke speed were adjusted for smooth, repeatable operation, and cylinder stroke timing was calibrated to meet precise actuation requirements.

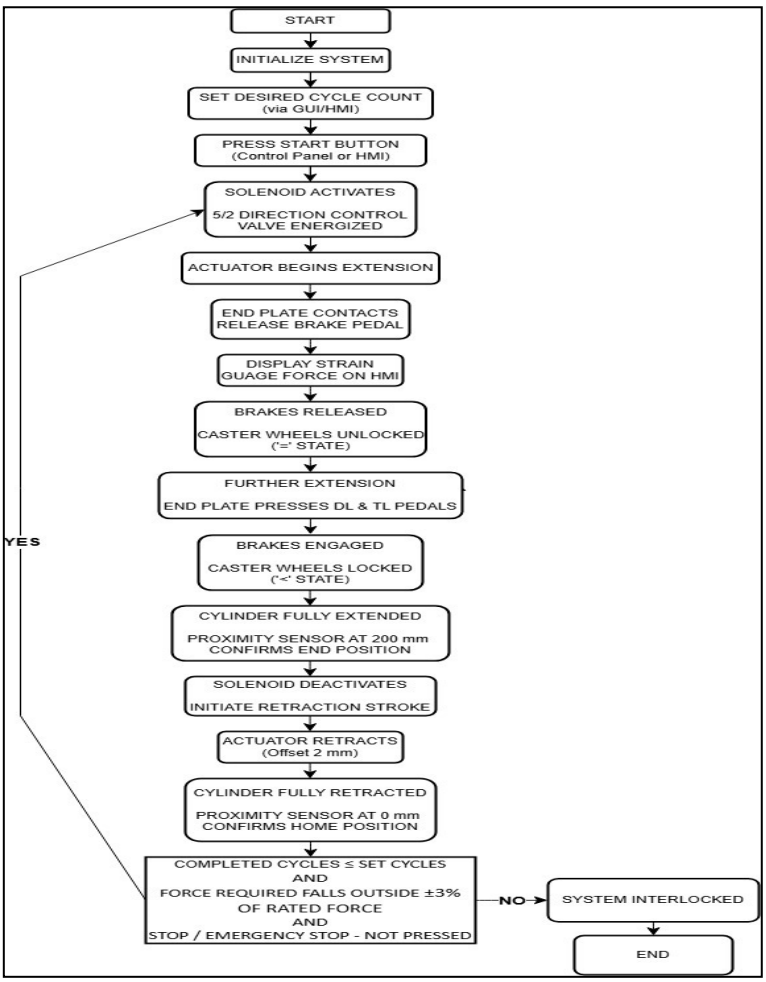

Fig. 7: Functional Flowchart of Test Cycle Logic Implemented in the PLC.

3. Results and discussion

The developed PLC-based automated test system was employed to evaluate the specified life cycle performance of the medical-grade caster wheel brake mechanism. The system functioned as intended over prolonged, unattended operations with continuous engagement-disengagement cycles for specified CL. This section presents the outcomes of force measurements, system responsiveness, and performance trends, followed by an interpretation of the results in the context of durability and mechanical behavior of the tested caster wheel brake mechanisms.

3.1. Functional validation of test setup

The test setup underwent a series of initial functional validation trials to confirm the proper operation and integration of its key subsystems, including pneumatic actuation, PLC logic execution, sensor feedback accuracy, and strain gauge force measurement.

The pneumatic actuator demonstrated stable and repeatable linear motion across its entire 200 mm stroke length, leading to dependable engagement and disengagement of the brake mechanism in each cycle. The proximity sensor, tasked with detecting the extended and retracted positions of the actuation plate, operated with complete accuracy, successfully registering end positions in all observed cycles and thereby ensuring both reliable cycle counting and enhanced operational safety.

To confirm the accuracy of the force values recorded through the strain gauge, a comparison was made with manually measured values obtained using a digital force gauge. Due to system limitations, it was not possible to measure both values simultaneously during the same cycle. Therefore, 100 manual measurements and 100 strain gauge recordings were collected independently under identical testing conditions. The mean value of the strain gauge recordings was then compared to the Mean of the manual measurements. Table 5 presents the summary of force requirements for both modes - manual measurement and automated test setup - recorded during the initial 200 trials. It was observed that the difference between the two mean values remained within ±1%. This small variation confirms that the strain gauge setup provides accurate and reliable force measurements concerning the manually measured reference values. This level of agreement validated the system's force-sensing reliability. Collectively, these observations confirmed that the automated test setup was functionally robust and well-suited for life cycle evaluation under repetitive mechanical loading and stress conditions.

3.2. Force measurement results

The force measurements were done for two phases: validation trials and actual accelerated testing.

3.2.1. Validation trials force measurement results

Figure 8 shows a sample recorded output of the strain gauge for one complete extension stroke corresponding to cycle no. 55 from the validation trials. The output graph of force clearly shows two peaks. The first peak force value of 93.57 N represents the disengagement force required to release the brakes. This occurs when the end plate reaches a position of 158 mm. The second peak force value of 83.97 N indicates the engagement force needed to apply the brakes and lock the caster wheel. This takes place when the end plate reaches a position of 200 mm. *Figure 8* clearly shows that the pedals are gradually pressed by the end plate, which is connected to the rod of the pneumatic actuator. The braking force was applied gently and uniformly during both engagement and disengagement. This confirms that the tuning of the force measurement system, based on the strain gauge output, is accurate. It also validates the smooth operation of the pneumatic actuator during the engagement and disengagement of the brakes through the pedals. It is interesting to note that the disengagement force is higher compared to the engagement force in caster wheel braking systems. The higher disengagement force compared to engagement force in caster wheel braking systems can be attributed to the mechanical locking mechanism, design intent for safety, and spring-loaded return resistance. Mechanically, many braking systems employ self-locking components that become more secure under load, requiring additional force to release. From a safety perspective, the design ensures that the brake remains firmly engaged and is not easily disengaged by accidental contact or vibrations, which is especially important in medical environments. Additionally, spring elements used to maintain brake engagement resist release, further contributing to the increased force required during disengagement.

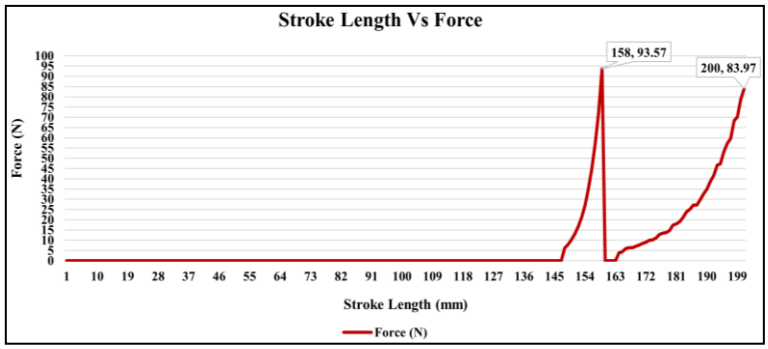

Fig. 8: Sample Recorded Output of Strain Gauge for One Complete Extension Stroke, Cycle No. 55.

Table 5 summarizes the force requirements for both modes (manual and recorded through automated test setup), confirming close alignment between manually observed and sensor-based measurements during the initial 200 trials. These trials helped to finalize the rated peak force values as 94.17 N for brake disengagement and 84 N for brake engagement. These served as reference-rated values for subsequent life cycle (C_L) testing. Any variation exceeding ±3% of the rated values, i.e., any deviation beyond 91.34 N and 96.99 N of brake disengagement force and 81.48 N and 86.52 N of brake engagement, is identified as abnormal.

It is important to note that the force typically required to operate medical caster wheel brakes (for engagement and disengagement of brakes) falls within 22–100 N, depending on caster design, load capacity, and brake mechanism. Some designs, such as cam-action tread locks, require minimal force - often operable with a light toe press. The caster wheel selected for this study conforms to this typical range, reinforcing the relevance of selected rated values [31-33]. *Figure 9* shows the variation in the peak force required on the release brake pedal for disengaging the brakes during the validation trials. *Figure 10* shows the variation in peak force required on the DL and TL brake pedals for engaging the brakes.

Sensor accuracy, especially from the strain gauge and proximity sensors, was validated through cross-verification to ensure reliable signal acquisition and feedback. PLC logic was refined to manage cyclic execution and fault detection efficiently, maintaining stable operation across all trials. In parallel, the system was observed for early signs of mechanical wear caused by repeated cycling, with no evidence of degradation affecting performance during the initial 200 trials. The mean engagement and disengagement force recorded through the test setup remained within a ±1% of manual measurements, affirming the system's robustness for long-term testing.

Table 5: Summary of Forces during Validation Trials

Description	Force required on the release brake pedals for disengagement of the brakes (Peak Value) in Newtons		Force required on the DL and TL brake pedals for engagement of the brakes (Peak Value) in Newtons	
	Measured	Recorded	Measured	Recorded
Minimum Force	93.22	93.23	83.16	83.20
Maximum Force	94.98	94.99	84.79	84.79
Mean Force	94.16	94.18	83.99	84.02
The rated force was decided for testing	94.17		84.00	
Minimum Rated Force for testing (–3%)	91.34		81.48	
Maximum Rated Force for testing (+3%)	96.99		86.52	

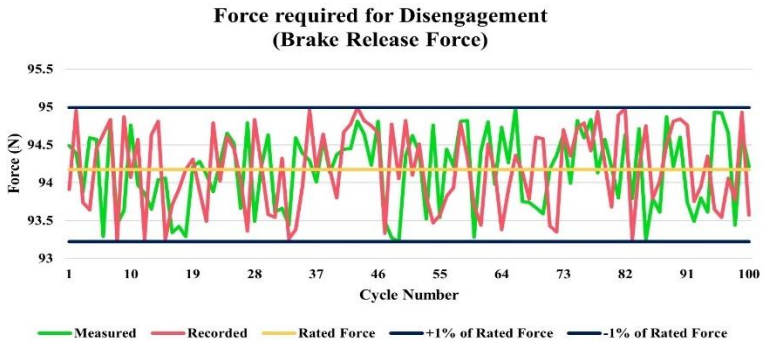

Fig. 9: Disengagement Force Measured Over 200 Validation Trials, comparing 100 Manually Acquired Measurements with 100 Strain-Gauge-Recorded Values from the Automated PLC-Based Test Setup.

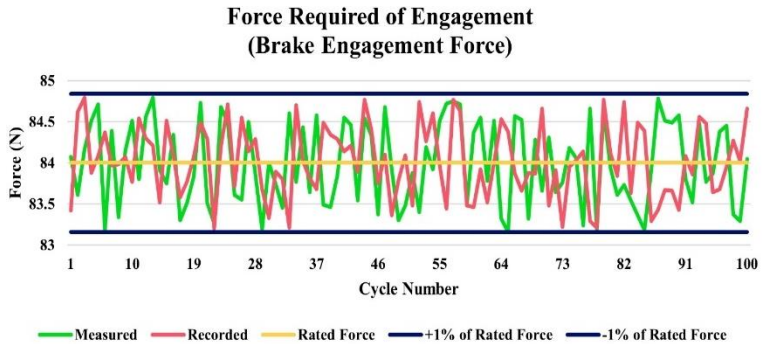

Fig. 10: Engagement Force Measured Over 200 Validation Trials, comparing 100 Manually Acquired Measurements with 100 Strain-Gauge-Recorded Values from the Automated PLC-Based Test Setup.

3.2.2. Statistical validation

A paired t-test analysis was conducted to determine the statistical significance of the validation trials' force measurement results for engagement forces and disengagement forces separately. The p-values obtained for manual and recorded force measurements of engagement and disengagement of brakes were $p > 0.05$, confirming that the mean values of both manual and recorded measurements for engagement as well as disengagement are similar. Table 6 presents the paired t-test results.

Table 6: Results of Paired T-Test for Manual and Recorded Force Measurements of Engagement and Disengagement of Brakes

Parameter	Description			
	Engagement		Disengagement	
P-value and statistical significance:	The two-tailed P value equals 0.6545 By conventional criteria, this difference is not statistically significant.		The two-tailed P value equals 0.8118 By conventional criteria, this difference is not statistically significant.	
Confidence interval:	The Mean of Measured Engagement Force minus the Recorded Engagement Force equals -0.0303 95% confidence interval of this difference: From -0.1642 to 0.1036		The Mean of Measured Disengagement Force minus the Recorded Disengagement Force equals -0.0161 95% confidence interval of this difference: From -0.1499 to 0.1177	
Intermediate values used in calculations	t = 0.4489 df = 99 Standard error of difference = 0.068		t = 0.2388 df = 99 Standard error of difference = 0.067	
Review of data used for the analysis:				
Group	Measured Engagement Force	Recorded Engagement Force	Measured Disengagement Force	Recorded Disengagement Force
Mean	83.9886	84.0189	94.163	94.1791
Standard Deviation	0.5063	0.44	0.5045	0.5337
Standard Error of the Mean	0.0506	0.044	0.0505	0.0534
Sample Size	100	100	100	100

3.2.2. Accelerated testing force measurement results

Force readings were recorded manually using a digital force gauge after specific intervals: 0, $0.1C_L$, $0.2C_L$,……., C_L. Both engagement (brake locking) and disengagement (brake releasing) forces were evaluated to assess caster wheel braking mechanism consistency and robustness over time. Table 7 shows the manual and recorded force measurements across C_L at specific intervals. The reader is requested to read Table 4 to understand the interval notations. *Figure 11* and *Figure 12* graphically represent the corresponding force trends for these measurements over the same intervals. It is seen that all the values (manual measurement as well as recorded through strain gauge) lie within the minimum and maximum rated force (i.e. ±3% of respective rated force) required for engagement and disengagement of the brakes of the caster wheel. Table 7 also shows the force variation trend w.r.t. the number of cycles completed. From 0 to 0.5 C_L, both manually measured values and those recorded through the strain gauge remained within ±1% of the respective rated forces. Between 0.5 C_L and C_L, all measured values stayed within ±2% of the rated forces. Instances where the deviation exceeded ±1% were observed but occurred less frequently. This confirms that the test setup is functioning properly and delivering reliable performance throughout the C_L. Although none of the measured values crossed the extreme boundary condition of ±3%, a clear trend of gradual deviation from the rated force values was observed as the cycle count approached C_L. This indicates that while the braking mechanism did not fail during the test, it showed signs of performance degradation.

The gradual and slight increase in force variation over the test cycles indicates the early onset of wear or changes in the behavior of the brake components. Throughout the test, the measured forces remained within the acceptable range, but a clear trend toward deviation from the rated values was observed as the cycle count approached C_L.

Table 7: Manual Force Measurement and Recorded Force Across Life Cycles at Certain Intervals

Sr. No.	Inter-val	Rated	Rated Minimum (–3%)	Man-ual	Rec-orded	Rated Maximum (+3%)	% variation w. r. t. Rated	Remark
1	0B	84.00	81.48	83.56	83.87	86.52	0.15	
2	1R	94.17	91.34	93.54	94.95	96.99	-0.83	
	1B	84.00	81.48	83.46	84.25	86.52	-0.30	
3	$0.1C_LR$	94.17	91.34	93.25	94.50	96.99	-0.35	
	$0.1C_LB$	84.00	81.48	83.20	84.22	86.52	-0.26	
4	$0.2C_LR$	94.17	91.34	93.26	94.20	96.99	-0.03	
	$0.2C_LB$	84.00	81.48	84.15	84.18	86.52	-0.21	Variation within ±1% of the respective rated force value
5	$0.3C_LR$	94.17	91.34	93.30	94.52	96.99	-0.37	
	$0.3C_LB$	84.00	81.48	83.26	84.27	86.52	-0.32	
6	$0.4C_LR$	94.17	91.34	93.50	94.68	96.99	-0.54	
	$0.4C_LB$	84.00	81.48	84.56	84.77	86.52	-0.92	
7	$0.5C_LR$	94.17	91.34	94.26	93.25	96.99	0.98	
	$0.5C_LB$	84.00	81.48	83.36	84.44	86.52	-0.52	
8	$0.6C_LR$	94.17	91.34	95.76	94.66	96.99	-0.52	
	$0.6C_LB$	84.00	81.48	84.66	85.06	86.52	-1.26	
9	$0.7C_LR$	94.17	91.34	95.06	94.86	96.99	-0.73	
	$0.7C_LB$	84.00	81.48	84.96	84.86	86.52	-1.02	
10	$0.8C_LR$	94.17	91.34	94.62	93.76	96.99	0.44	Variation within ±2% of the respective rated force value
	$0.8C_LB$	84.00	81.48	84.26	83.36	86.52	0.76	
11	$0.9C_LR$	94.17	91.34	94.55	93.36	96.99	0.86	
	$0.9C_LB$	84.00	81.48	83.66	85.02	86.52	-1.21	
12	C_L	94.17	91.34	94.34	94.76	96.99	-0.63	
	C_L	84.00	81.48	84.56	83.92	86.52	0.10	

Note: The Reader is advised to read Table 4 to understand the interval notations.

This trend suggests that the braking mechanism is approaching its performance limit. Although the variation did not exceed the ±3% threshold, it is reasonable to expect that continued testing beyond C_L - possibly up to $2C_L$ or more - could lead to exceeding this limit. However, this assumption cannot be confirmed within the current study, as testing was not extended until failure and is beyond the scope of this study.

Based on these observations, the data support confirming C_L as the functional life of the caster wheel brake mechanism under the defined conditions. While failure was not observed, the increasing trend toward deviation indicates a shift toward the permissible threshold. This reinforces the conclusion that the brake mechanism is reliable up to C_L and performs its intended function effectively within this tested lifecycle.

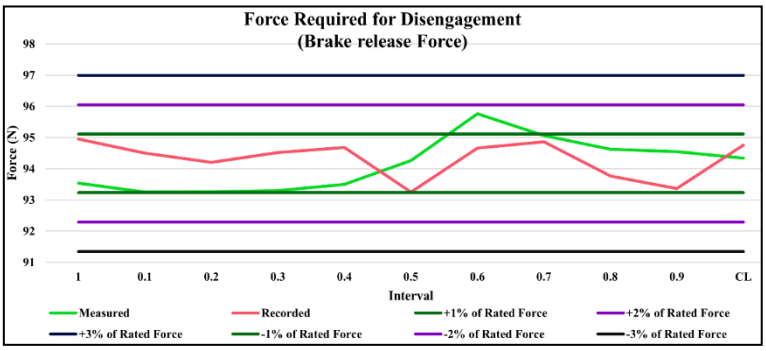

Fig. 11: Line Chart Showing Force Required for Disengagement Measured at Specific Intervals Over C_L, Highlighting Variations in Trends of Force Required Throughout the C_L.

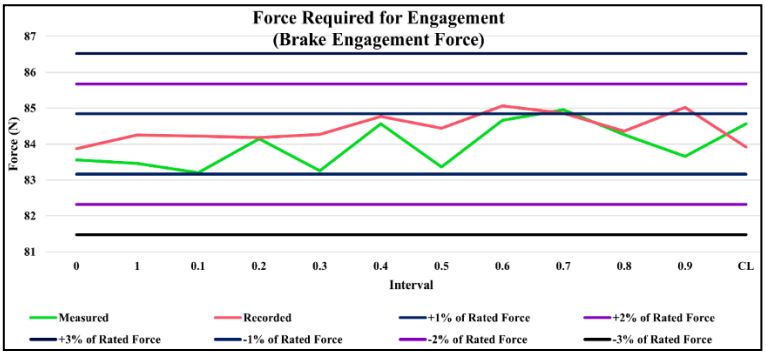

Fig. 12: Line Chart Showing Force Required for Engagement Measured at Specific Intervals Over C_L, Highlighting Variations in Trends of Force Required Throughout the C_L.

3.3. Analysis of engagement force (lock state)

The recorded engagement force exhibited remarkable consistency over the life cycle C_L duration. The initial force at 0 cycle was 83.87 N and showed a minor increase and fluctuation during intermediate readings. The force value slightly rose to 85.06 N at $0.6C_L$ cycles and showed minor fluctuation until C_L, with a final reading of 83.92 N at C_L cycles. The variation remained within ±3% of the rated value.
These results indicate that the brake engagement mechanism maintained consistent functionality throughout the entire test duration. The slight increase and fluctuation observed midway through the cycle count are expected due to normal mechanical settling, material fatigue, or slight wear in the brake components. However, the fact that all recorded values remained within ±3% of the rated engagement force confirms that the system did not exhibit any significant degradation or deviation.
Additionally, the pneumatic system demonstrated uniform actuation characteristics, ensuring consistent contact between the actuator plate and the brake lever throughout the testing cycles. The strain gauge also maintained stable performance over extended usage, showing no signs of signal drift, thereby reinforcing the reliability of sensor feedback for long-duration tests. The minimal deviation indicated the structural durability of the caster brake mechanism under cyclic stress conditions commonly encountered in medical devices.
This consistency supports the conclusion that the engagement performance of the caster wheel brake remains within acceptable limits over its tested life span and validates the durability of the design under the given test conditions.

3.4. Analysis of disengagement force (unlock state)

The recorded disengagement force began at 94.95 N at the first cycle and experienced a slight decrease to 93.25 N at $0.5C_L$. This was followed by a steady increase, reaching 94.86 N at $0.7C_L$ cycles. Further again a steady decrease was observed to 93.36 N at 0.9 C_L. However, all these values fell within ±3% of the rated value.
These fluctuations are minor and remain well within the ±3% tolerance range of the rated disengagement force, indicating no abnormal wear or sudden shift in mechanical behavior. The alternating pattern of increase and decrease suggests a stable but responsive system that may be adjusting slightly due to mechanical settling, minor component deformation, or variations in surface friction under repeated cycling.
During the early cycles, internal brake components undergo a bedding-in phase, leading to slight variations in frictional resistance. This is accompanied by subtle realignment within the disengagement linkage, likely due to microscopic positional shifts as the components settle into their operational paths.
Additionally, mechanical elements appear to reach a steady state after a brief run-in period, contributing to the overall consistency observed in subsequent cycles. Unlike engagement, which relies heavily on static pressure, disengagement may involve a combination of spring return, reduced preload, and dynamic unbinding of brake components. Despite these factors, the force required remained well within acceptable tolerance limits.
Importantly, the absence of any sharp or progressive deviation supports the conclusion that the disengagement mechanism remains functionally reliable over the tested life span. The data confirms that the braking system maintains its ability to release properly without requiring significantly higher or lower forces, which is crucial for safe and predictable operation, especially in medical equipment applications.

3.5. System responsiveness and reliability

The PLC-controlled automation system demonstrated uninterrupted performance throughout all validation trials as well as testing cycles, functioning without any software or mechanical issues. The integrated feedback loop comprising proximity sensors and a strain gauge enabled precise regulation of proper actuator stroke and accurate force measurements. The automation ensured high operational fidelity, with the cycle counting mechanism achieving over 100% accuracy and no instances of missed cycles. Emergency stop protocols were activated at multiple checkpoints, confirming the reliability of the system's fault-handling capabilities during validation trials. Additionally, the analog signal conditioning circuitry maintained stable, noise-free readings even during extended operation. These outcomes affirm the system's suitability for real-time accelerated life testing applications, where autonomous monitoring, actuation, and performance evaluation of test components are essential.

3.6. Practical implications

The developed test system presents significant advantages for both the healthcare industry and medical device manufacturers. Its ability to perform accelerated lifecycle testing enables rapid assessment of mechanical components, significantly shortening the time required to evaluate durability and reliability. High repeatability in test cycles ensured the extended applicability of the methodology and developed a test setup for consistent and comparable results across different caster wheel models, facilitating informed product selection and benchmarking. The integration of strain-based monitoring along with the PLC-based automated test setup provides valuable insights by identifying early signs of mechanical fatigue, allowing for proactive design improvements. Additionally, the incorporation of automation and a user-friendly graphical interface minimizes manual intervention, thereby reducing labor demands and eliminating the potential for human error during testing.

3.7. Scope of testing conditions

While the present study successfully demonstrates a reliable PLC-based automated test system for evaluating caster wheel brake mechanisms, the scope of the experimental conditions is intentionally limited to static configurations with linear loading. Dynamic influences, such as cyclic variations in force during rolling, rotational loading of the caster assembly, and transient impact forces encountered in actual hospital environments, were not incorporated. Similarly, environmental parameters—including variations in temperature, humidity, and exposure to cleaning chemicals —were beyond the scope of the current setup. These factors can influence material properties, wear rates, and brake performance over time.
However, by the operational guidelines provided in the relevant manufacturer manuals [34-36], all tests were performed in a controlled environment with relative humidity maintained between 15% and 95% RH and temperature between 10 °C and 60 °C, which aligns with the intended use conditions of the medical caster wheel assemblies.
Future iterations of the system will aim to integrate multi-axis actuation for simulating rotational and lateral forces, along with environmental chambers to replicate real-world operational conditions. Such advancements would enable a more holistic evaluation of brake

mechanisms under diverse service scenarios, further enhancing the system's applicability for predictive maintenance and quality assurance in medical device manufacturing.

3.8. Practical challenges, enhancements, and implementation pathways

The developed automated caster wheel brake testing system demonstrates robust reliability, maintaining functionality within ±3% of rated forces across repeated test cycles. Its automation capability minimizes operator dependency, reduces testing time, and improves repeatability. However, practical deployment presents certain challenges. For instance, adapting the system for dynamic testing would require simulating real-world rolling conditions, including varying surface textures, gradients, and load transitions. Additionally, integrating IoT-enabled sensors could facilitate real-time monitoring, predictive maintenance, and remote diagnostics. Such enhancements could also improve traceability for quality audits and compliance with regulatory standards. Furthermore, implementing a modular control architecture would support adaptability for testing other mechanical assemblies beyond caster wheel brakes.

4. Conclusion

This research successfully presents the design and development of a PLC-based automated test system for the life cycle evaluation of caster wheel brake mechanisms used in medical equipment. The primary aim was to create a robust, repeatable, and efficient method to simulate operational conditions and monitor mechanical performance across many engagement-disengagement cycles of the braking mechanism of the caster wheel.

The results demonstrated that the test setup reliably performed for C_L uninterrupted cycles while capturing essential mechanical data through strain gauge feedback and proximity sensor validation. The Caster Wheel under study showed negligible force degradation, with average force values remaining within a ±3% tolerance throughout the test period. This consistency confirms the mechanical reliability and long-term durability of the braking system, validating both the test setup and the product design.

The integration of PLC control with a pneumatic actuator and real-time force monitoring allowed for high-precision cyclic testing with minimal human intervention, significantly improving testing speed and reducing labor costs. The system's ability to run unattended, accurately, and safely positions it as an asset for quality assurance and R&D testing in medical equipment manufacturing.

The findings of this study confirm that the developed automated testing setup for caster wheel brake mechanisms consistently maintains performance within ±3% of the rated forces over the specified C_L cycles. By addressing a critical gap in the domain of automated testing for caster wheel brakes, the proposed system not only ensures repeatable and reliable performance assessment but also offers tangible benefits in terms of operational efficiency. From a regulatory compliance perspective, the system's ability to produce accurate, traceable test data supports adherence to industry and safety standards, thereby facilitating certification processes. Economically, the automation of the testing procedure reduces labor dependency, minimizes human error, and shortens testing cycles, resulting in significant cost savings over time. Furthermore, the modular design of the setup enables scalability and adaptability for testing a variety of mechanical components beyond caster wheel brakes, extending its potential application to broader manufacturing and maintenance contexts. These combined advantages position the system as a valuable contribution to the ongoing shift toward Industry 4.0 practices in quality assurance and smart manufacturing environments.

4.1. Limitations

Despite the high level of repeatability and automation achieved by the developed test system, several limitations must be acknowledged. Force readings, although reliable, were manually verified at defined intervals rather than continuously logged, due to current hardware limitations intended to maintain system robustness. The system replicates only linear loading conditions and does not account for dynamic forces, rotational movement, or predefined force profiles typically encountered in real-world applications. Moreover, the test simulates the caster wheel in a static state without replicating rolling or directional changes under load. Environmental factors such as ambient temperature and humidity— which can significantly influence material fatigue and wear—were not actively controlled or monitored during the test process.

The present investigation was limited to the predetermined cycle life (C_L) as per the approved test plan and project scope, which were defined to meet contractual deliverables and resource constraints. Post-C_L testing was therefore not conducted, as the primary objective of this phase was to validate performance within the specified operational lifespan rather than to evaluate end-of-life behavior. Consequently, the study does not capture the progression of wear or other degradation phenomena beyond the designated operating duration. Extending the analysis to include failure testing and detailed examination of components —as microscopic inspection, material characterization, or wear debris analysis—would provide valuable insights into the mechanisms leading to performance deterioration or ultimate failure. Future work will incorporate such evaluations to establish a more complete understanding of potential failure modes and their implications for design improvement and maintenance planning.

4.2. Future scope

Future improvements and research directions can focus on addressing the current limitations and expanding the capabilities of the test system. One key enhancement would be the inclusion of dynamic loading conditions and variable resistance, which would allow more realistic simulation of the actual operating environment faced by medical carts and devices. This approach can better reflect the complex stresses acting on caster wheel braking systems [37].

Another important area for future work is estimating the travel distance of caster wheels over the equipment's life cycle, enabling the correlation between cumulative wear and braking force. This can provide valuable insights into long-term brake performance.

Expanding the test framework to accommodate caster wheels from different manufacturers and design configurations would also enable comprehensive comparative analysis, improving the generalizability of the results.

Additionally, incorporating IoT-based real-time data acquisition systems could support continuous monitoring of force, cycle count, and early failure detection, enhancing both precision and traceability. This direction aligns with ongoing efforts in smart manufacturing and digital transformation [38].

The developed automated caster wheel brake testing system demonstrates significant potential for enhancing reliability, consistency, and efficiency in mechanical endurance evaluation. While the current setup is optimized for static and cyclic load testing, practical challenges

remain in extending its applicability to dynamic testing scenarios. Future work could involve the incorporation of programmable servo-actuators or cam-based mechanisms to simulate realistic rolling conditions and multi-directional forces encountered in service environments. Integrating Internet of Things (IoT) modules with wireless data transmission and cloud-based analytics could enable real-time monitoring, predictive maintenance alerts, and remote performance verification, thereby improving operational decision-making. Additionally, quantitative studies on cost–benefit analysis—considering reduced labor, faster testing cycles, and enhanced compliance with international safety regulations—would further validate the system's industrial value. Scaling the methodology to test other wheeled components, such as hospital bed castors, trolley wheels, and heavy-duty industrial rollers, could broaden its applicability. Furthermore, planned research on accelerated failure analysis and adaptive load profiling will help identify early warning indicators, improving preventive maintenance strategies and product lifecycle management.

4.3. Academic contribution

Academically, this study exemplifies the practical application of mechatronics and automation in the field of mechanical component life testing, an area often limited to manual or partially automated approaches. The work establishes a replicable test methodology suitable for educational laboratories and research facilities focused on automated testing, medical device design, and reliability engineering.

4.4. Research contribution

From a research perspective, the developed test system offers a validated approach to endurance testing using a PLC-based framework integrated with smart sensors for feedback and control. It provides quantitative insights into the durability of medical caster brake mechanisms under repeated actuation. Additionally, the modular and scalable nature of the system makes it adaptable for testing other mechanical subassemblies - such as hinges, latches, or linear actuators - under cyclic stress conditions.
In summary, the PLC-driven automated test platform demonstrates a cost-effective, technically sound, and scalable solution for life cycle evaluation of mechanical components used in medical applications. The findings not only confirm the mechanical reliability of the brake mechanism but also emphasize the broader applicability of such systems in modern, automated reliability testing environments.
Moreover, applying accelerated degradation modeling (digital transformation and predictive modeling) can help predict long-term behavior using short-duration tests, while the current setup can also be extended to support Failure Mode and Effects Analysis (FMEA) and Failure Mode, Effects, and Criticality Analysis (FMECA) for reliability assessment. The concept of such digital extensions has been explored by many researchers [39-41].

5. Glossary

Caster Wheel: A wheel that can rotate in any direction. It's commonly used under carts, chairs, or medical equipment to allow easy movement.
Ethernet: A wired technology used to connect devices to a network, such as connecting a PLC or computer to a control system.
GUI (Graphical User Interface): A visual interface with buttons, icons, and graphics that makes software easy to use, like what you see on a smartphone or computer screen.
HMI (Human-Machine Interface): A screen or panel that lets people interact with machines, showing data and allowing manual input (like start/stop buttons).
IoT (Internet of Things): IoT is about making objects "smart" by connecting them to the internet so they can talk to each other and to us. It connects everyday physical objects like machines, appliances, or sensors to the internet so they can send, receive, and share data without human involvement.
ML (Machine Learning): Machine Learning is a branch of artificial intelligence where computers learn from data to make predictions or decisions without being explicitly programmed for every step.
PLC (Programmable Logic Controller): An industrial computer used to control machines and processes in industrial settings. It automates tasks like turning on/off or reading sensor data.
Pneumatics: A technology that uses compressed air to power mechanical systems. It's often used to move or control parts of a machine.
Proximity Sensor: A sensor that detects when an object is nearby without touching it. Commonly used to detect position or movement in machines.
Smart Manufacturing: Smart Manufacturing is the use of advanced technologies like IoT, artificial intelligence (AI), robotics, and data analytics to make manufacturing processes more efficient, flexible, and automated.
Strain Gauge: A small device that measures how much something is stretching or compressing. It's often used to detect force or pressure. It works by detecting tiny changes in its electrical resistance when the object it is attached to changes shape. This is often used to measure force, weight, or pressure.

References

[1] Maria Luisa Toro, Emily Bird, Michelle Oyster, Lynn Worobey, Michael Lain, Samuel Bucior, Rory A. Cooper and Jonathan Pearlman, Development of a wheelchair maintenance training programme and questionnaire for clinicians and wheelchair users, *Disability and Rehabilitation: Assistive Technology*, vol. 12, issue 8, Jan 2017, pp. 843-851, https://doi.org/10.1080/17483107.2016.1277792.
[2] Alexandria M. James, Gede Pramana, Richard M. Schein, Anand Mhatre, Jonathan Pearlman, Matthew Macpherson, and Mark R. Schmeler, A descriptive analysis of wheelchair repair registry data, *Assistive Technology*, vol 35, issue 4, Mar 2022, pp. 1-9. https://doi.org/10.1080/10400435.2022.2044407.
[3] Anand Mhatre, Carmen DiGiovine, Alyssa Boccardi, Fangzheng Wu, and Bryan Hess, Ultralight wheelchair part failures are associated with sensor-monitored road shocks: A pilot study, *Assistive Technology*, vol. 37, issue 2, Jan 2025, pp. 135-144, https://doi.org/10.1080/10400435.2024.2448178.
[4] Ephrem Ryan Alphonsus, and Mohammad Omar Abdullah, A review on the applications of programmable logic controllers (PLCs), *Renewable and Sustainable Energy Reviews*, vol. 60, Jul 2016, pp. 1185-1205, https://doi.org/10.1016/j.rser.2016.01.025.
[5] Anand Mhatre, Joseph Ott, Jonathan Pearlman, Development of wheelchair caster testing equipment and preliminary testing of caster models, *African Journal of Disability*, vol. 6, Sep 2017, a358, https://doi.org/10.4102/ajod.v6i0.358.
[6] Anand Mhatre, Norman Reese, and Jonathan Pearlman, Design and evaluation of a laboratory-based wheelchair castor testing protocol using community data, *PLoS One*, vol. 15, issue 1, Jan 2020, article no. e0226621, https://doi.org/10.1371/journal.pone.0226621.

[7] Eliška Cézová, František Lopot, Martin Machac, and Josef Kamenický, Experimental measurements on a stand for a grain sampler, *Manufacturing Technology*, vol. 22, issue 4, Jul 2022, pp. 401-407, https://doi.org/10.21062/mft.2022.047.

[8] Jack J. Fried, Jonathan L. Pearlman, and Anand A. Mhatre, Accelerated wear testing shows that thermoplastic bushings could be a cost-effective and durable alternative to traditional bearings for wheelchair caster use, *Journal of Rehabilitation and Assistive Technologies Engineering*, vol. 9, Dec 2022, https://doi.org/10.1177/20556683221144805.

[9] Maneetkumar Dhanvijay, Rohit Patki, and BharatkumarAhuja, Development of PLC-Based Controller for Door Slam Platform, *Frontiers of Mechanical and Industrial Engineering: Optimization Methods for Engineering Problems*, Editors: Dilbagh Panchal, Prasenjit Chatterjee, Mohit Tyagi, and Ravi Pratap Singh, Chapter 2, (2023), pp. 17-30, Apple Academic Press, available at: https://www.taylorfrancis.com/chapters/edit/10.1201/9781003300731-2/development-plc-based-controller-door-slam-platform-maneetkumar-dhanvijay-rohit-patki-ahuja. https://doi.org/10.1201/9781003300731-2.

[10] Maneetkumar Dhanvijay, Vinay Kulkarni, Nitin Patil, and Anand Bewoor, Development of PLC-based system for lift gate slam platform, *Proceedings of The International Conference on Materials for Emerging Technologies: ICMET-2021*, 18–19 February 2022, Phagwara, India, AIP Conference Proceedings, vol. 2800, issue 1, Sep 2023, article No. 020231, https://doi.org/10.1063/5.0163916.

[11] V. Biagini, P. Bolognesi, G. Mechler, O. Frantisek, C. Simonidis and A. Delpozzo, Multi-domain mechatronic approach for the design of a vacuum contactor actuation drive, *2016 XXII International Conference on Electrical Machines (ICEM*), Lausanne, Switzerland, 2016, pp. 1126-1131, https://doi.org/10.1109/ICELMACH.2016.7732666.

[12] Mohd Javaid, Abid Haleem, Shanay Rab, Ravi Pratap Singh, and Rajiv Suman, Sensors for daily life: A review, *Sensors International*, vol. 2, Jul 2021, article No. 100121, https://doi.org/10.1016/j.sintl.2021.100121.

[13] Bartomeu Mora, Jon Basurko, Urko Leturiondo, and Joseba Albizuri, Strain virtual sensing applied to industrial presses for fatigue monitoring, *Sensors*, vol. 24, issue 11, May 2024, article no. 3354, https://doi.org/10.3390/s24113354.

[14] Yadhunandan D, and Vinodkumar H P, Design and development of PLC controlled pneumatic pressing system, *International Journal of Engineering Research & Technology (IJERT)*, vol. 12, issue 12, Dec 2023, article no. IJERTV12IS120057, Available at: https://www.ijert.org/research/design-and-development-of-plc-controlled-pneumatic-pressing-system-IJERTV12IS120057.pdf.

[15] M. Jiménez, E. Kurmyshev, and C. E. Castañeda, Experimental study of double-acting pneumatic cylinder, *Experimental Techniques*, vol. 44, Feb 2020, pp. 355-367, https://doi.org/10.1007/s40799-020-00359-8.

[16] Gorazd Fajdiga, Denis Rajh, Drago Vidic, and Bojan Gospodarič, The development of pneumatic fatigue test rig for wood-based specimens, *Forests*, vol. 11, issue 11, Nov 2020, article no. 1187, https://doi.org/10.3390/f11111187.

[17] Jaydeep N. Mane, Vikrant S. Shinde, Devendra B. Bhatia, Kiran B. More, V. D. Jadhav, and Govind A. Lele, "Caster Wheel Endurance Testing Rig", IOSR Journal of Mechanical and Civil Engineering (IOSR-JMCE), Volume 13, Issue 3 Ver. VII (May- Jun. 2016), PP 29-35. Available at: https://www.iosrjournals.org/iosr-jmce/papers/vol13-issue3/Version-7/E1303072935.pdf.

[18] Joseph Ott, and Jonathan Pearlman, "A scoping review of the rolling resistance testing methods and factors that impact manual wheelchairs", Journal of Rehabilitation and Assistive Technologies Engineering, Volume 8, Article No. 2055668320980300, January 2021. https://doi.org/10.1177/2055668320980300.

[19] Jernej Klemenc, Jure Kajbič, "Design of Accelerated Fatigue-Life Tests Based on Finite-Element Simulations and the Theory of Critical Distances", in Advances in Accelerated Testing and Predictive Methods in Creep, Fatigue, and Environmental Cracking, Eds. Kamran Nikbin, Zhigang Wei, and Sreeramesh Kalluri, ASTM International, 100 Barr Harbor Drive, PO Box C700, West Conshohocken, PA 19428-2959, 2023, pp. 187–205, https://doi.org/10.1520/STP164320210089.

[20] Simone Venturini, Carlo Rosso, and Mauro Velardocchia, "An automotive steel wheel digital twin for failure identification under accelerated fatigue tests", Engineering Failure Analysis, Volume 158, April 2024, Article No. 107979. https://doi.org/10.1016/j.engfailanal.2024.107979.

[21] Jon Arrizabalaga Aguirregomezcorta, "MPC based Caster Wheel Aware Motion Planning for Differential Drive Robots", Degree Project in Mechanical Engineering, School of Industrial Engineering and Management, KTH Royal Institute of Technology, 2020. Available at: https://www.diva-portal.org/smash/get/diva2:1469258/FULLTEXT01.pdf.

[22] Oded Medina, and Shlomi Hacohen, "Overcoming Kinematic Singularities for Motion Control in a Caster Wheeled Omnidirectional Robot", Robotics, Volume 10, No. 4, December 2021, Article No. 133, https://doi.org/10.3390/robotics10040133.

[23] K. Alapure, S. Chalke, R. Khadape and J. Gole, "Analytical Study of PLC and Microcontroller Based Parking System," 2023 9th International Conference on Electrical Energy Systems (ICEES), Chennai, India, 2023, pp. 221-225, https://doi.org/10.1109/ICEES57979.2023.10110248.

[24] Wenhao Yan, Jing Wang, Shan Lu, Meng Zhou and Xin Peng, "A Review of Real-Time Fault Diagnosis Methods for Industrial Smart Manufacturing", Processes, Volume 11, No. 2, January 2023, Article No. 369, https://doi.org/10.3390/pr11020369.

[25] Embong, A. & Asbollah, L. & Hamid, S. (2024). Empowering industrial automation labs with IoT: A case study on real-time monitoring and control of induction motors using Siemens PLC and Node-RED. Journal of Mechanical Engineering and Sciences. https://doi.org/10.15282/jmes.18.2.2024.3.0790.

[26] Pawar, Shital & Kanjalkar, Pramod & Londhe, Aditya & Gite, Vaishnavi & Wabale, Snehal. (2025). PLC Diagnosis and Monitoring System. 1481-1488. https://doi.org/10.1109/ICICT64420.2025.11005035.

[27] Taimun, Md & Sharan, S M Mobasshir Islam & Azad, Md Ashraful & Joarder, Md. (2025). Smart Maintenance and Reliability Engineering in Manufacturing. Saudi Journal of Engineering and Technology. 10. 189-199. https://doi.org/10.36348/sjet.2025.v10i04.009.

[28] M. J. Dixon, Dynamic force measurement, In: Dyson, B.F., Loveday, M.S., Gee, M.G. (eds) *Materials Metrology and Standards for Structural Performance*. Springer, Dordrecht, 1995, https://doi.org/10.1007/978-94-011-1264-2_4.

[29] Tingwei Gu, Shengjun Yuan, Lin Gu, Xiaodong Sun, Yanping Zeng, and Lu Wang, Research on dynamic calibration and compensation method of strain-gauge type force sensor, *Sensor Review*, vol. 44, issue 1, Jan 2024, pp. 68-80. https://doi.org/10.1108/SR-08-2023-0330.

[30] Andrea Prato, Alessio Improta, Michele Di Lernia, Salvatore Nobile, Alessio Facello, Fabrizio Mazzoleni, Alessandro Germak, and Alessandro Schiavi, Static, continuous and dynamic calibration of force transducers: A comparative study on a low-force strain-gauge measuring device, *Measurement: Sensors*, vol. 38, supplement, May 2025, article no. 101337, https://doi.org/10.1016/j.measen.2024.101337.

[31] The Ergonomics of Manual Material Handling Pushing and Pulling Tasks. Whitepaper by Darcor Casters and Ergoweb, Conveyer and Caster Corporation, 2001. Available at: https://www.cc-efi.com/wp-content/uploads/2018/08/Darcor_Whitepaper.pdf.

[32] Test Report No. BR –151/L-274/2009, Polish Centre for Testing and Certification, 02-699 Warszawa, ul. Kłobucka 23A, Mechanical Laboratory, 2009, Available at: https://hmi-basen.dk/blobs/testrapporter/96820_76.pdf.

[33] Report: Vocabulary, Performance and Testing Requirements for Casters and Wheels, Institute of Casters and Wheel Manufacturers, An Industry Group of MHI, ANSI ICWM-2018 revision of ANSI ICWM-2012, 2018, Available at: https://nwcaster.com/wp-content/uploads/2020/08/ICWM-Caster-Testing-Requirements.pdf.

[34] Vivid S70 / S60 – User Manual i-3 BC092860-1EN 01, User Manual By GE Medical Systems, Available at: https://www.gehealthcare.com/support/manuals?srsltid=AfmBOooK16F910Yq6ubmuW2lluYfMCGRXGp-loyg1u9Vkqp3yTygqNge&search=eyJzZWFyY2hUZXJtIjoiQkMwOTI4NjAtMUVOIiwibGFuZ3VhZ2VOYW1lIjoiRW5nbGlzaCAoRU4pIn0%3D.

[35] Venue R2 Basic User Manual – EN, User Manual By GE Medical Systems, Available at: https://www.gehealthcare.com/support/manuals?srsltid=AfmBOooK16F910Yq6ubmuW2lluYfMCGRXGp-loyg1u9Vkqp3yTygqNge&search=eyJzZWFyY2hUZXJtIjoiNTc5NDg0MS0xMDAiLCJsYW5ndWFnZU5hbWUiOiJFbmdsaXNoIChFTikifQ%3D%3D.

[36] EPIQ 7 Ultrasound System User Manual, Available at: https://usme.com/wp-content/uploads/2022/06/epiq_7.pdf.

[37] S. M. Patil and B. B. Ahuja, Tribological behaviour of PTFE under variable loading dry sliding condition, *Journal of the Institution of Engineers (India): Series C*, vol. 95, Apr 2014, pp. 179–185. https://doi.org/10.1007/s40032-014-0106-4.

[38] Prathamesh S. Shinde, Chaitanya Shrikant Poredi, Ganesh Suresh Shelke, Srishti Sudhir Patil, Jahida Javed Subhedar, Maneetkumar Rangnath Dhanvijay, Sudhir Madhav Patil, Transforming MSME assembly operations: smart manual assembly table for improved productivity, *International Journal of Basic and Applied Sciences (IJBAS)*, vol. 14, issue 1, Apr 2025, pp. 40-51, https://doi.org/10.14419/am35a906.

[39] Akshay Dattaprasad Khamkar, Sudhir Madhav Patil, Digital Twin in Fluid Power: Reviewing Constituents, *International Research Journal of Multidisciplinary Scope (IRJMS)*, vol. 5, issue 1, Jan 2024, pp. 750-765, https://doi.org/10.47857/irjms.2024.v05i01.0365.

[40] Akshay Dattaprasad Khamkar, Sudhir Madhav Patil, Digital Twin in Fluid Power: Review- Technology Trends, *International Research Journal of Multidisciplinary Scope (IRJMS)*, vol. 5, issue 2, Apr 2024, pp. 596-610, https://doi.org/10.47857/irjms.2024.v05i02.0586.

[41] Akshay Dattaprasad Khamkar, Sudhir Madhav Patil, Digital Twin in Fluid Power: Review – Uses and Outlook, *International Research Journal of Multidisciplinary Scope (IRJMS)*, vol. 5, issue 3, Jul 2024, pp. 79-96, https://doi.org/10.47857/irjms.2024.v05i03.01085.